ACTA SCIENTIARUM POLONORUM *Architectura 3 (1) 2004, 77–92*

THE EULER'S MODIFIED THEORY OF STABILITY WITH STRESSES AND STRAINS ANALYSIS ON EXAMPLE OF VERY SLENDER CYLINDRICAL SHELLS MADE OF STEEL

Krzysztof Murawski

Abstract. The study presents the description of the loss of stability in elastic states of axially compressed cylindrical shell. The author analysed the differential equation of the deflection curve and its slope, the critical stress, the shell stresses and strains of very slender tubes in elastic states under conditions of flat cross-sections and little slopes of the deflection curve. The obtained theoretical results of critical stresses were related to slenderness ratio and to cross-section area of the cylindrical shells. The obtained theoretical results of stresses and strains were presented on graphs for an example of the tube made of steel.

Key words: stability, Euler, critical stress, very slender, cylindrical shell

STABILITY ANALYSIS

The basic theory of slender rod losing stability in elastic states was formulated by Euler [1744, 1759]. He introduced the concept of critical load and gave, according to his theory, the formulas for the differential equation of the deflection curve and for critical stress of axially compressed rod:

$$EJ\frac{d^2y}{dx^2} = P_{cr}y \quad , \quad \sigma_{cr}^{Euler} = \left(\frac{\pi}{\lambda}\right)^2 E \tag{1}$$

where: P_{cr} – the critical force,
E –Young's modulus of elasticity of rod,
J – moment of inertia of cross-section area,
σ_{cr} – critical stress,
λ – slenderness ratio.

This theory was developed during next years by Grashof [1878], Considère [1889], Salmon [1921], Bleich [1952], Timoshenko and Gere [1963], Březina[1966], Wolmir [1967], Życzkowski [1981], Grigoliuk and Kabanow [1987], Weiss and Giżejowski [1991], Reese and Wriggers [1995] and many others.

The author assumed in his own analysis of rods stability [Murawski 1992, 1998, 2002], that the state of stresses in the critical transverse section, after losing stability and before losing carrying capacity, is as the result of a superposition of pure compression and bending (Fig. 1 and 2) and the start of losing of a carrying capacity (the maximum force on a force-shortness graph) in elastic states follows after the exit of the resultant neutral layer from the critical transverse section. In this paper has assumed as a simplification for very slender columns, that the start of loss of a carrying capacity follows after the exit forces line from the critical transverse section.

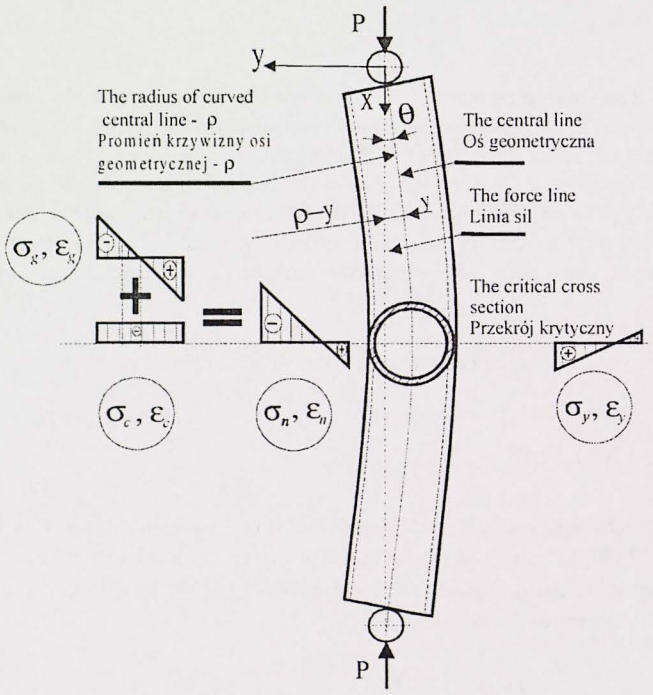

Fig. 1. The state of normal stresses of tube axially compressed with forces by balls, in the critical transverse section caused by external and internal load, after losing of stability and before losing carrying capacity, according to author's hypothesis

Rys. 1. Stan naprężeń normalnych rury osiowo ściskanej siłami przez kule w krytycznym przekroju poprzecznym powodowany przez zewnętrzne i wewnętrzne obciążenie, po utracie stateczności i przed utratą nośności, zgodnie z hipotezą autora

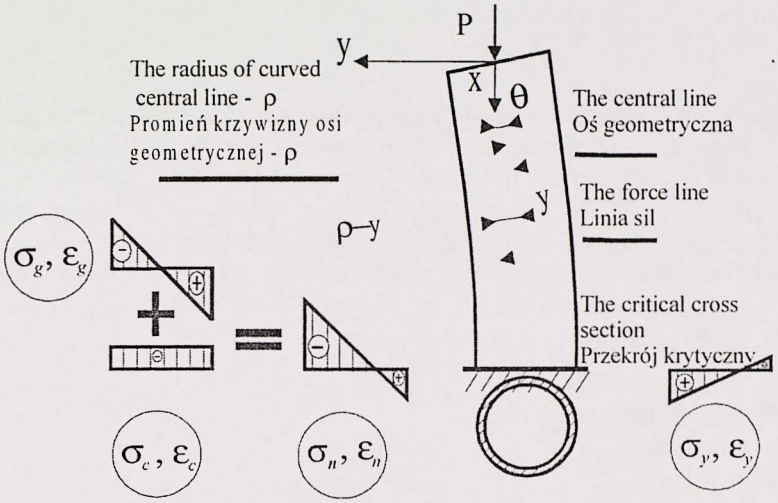

Fig. 2. The state of normal stresses of axially compressed tube with one end fixed, in the critical transverse section, caused by external and internal load, after losing of stability and before losing carrying capacity, according to author's hypothesis
Rys. 2. Stan naprężeń normalnych osiowo ściskanej rury utwierdzonej w jednym końcu w krytycznym przekroju poprzecznym, powodowany przez zewnętrzne i wewnętrzne obciążenie, po utracie stateczności i przed utratą nośności, zgodnie z hipotezą autora

The extension of any fibre at the distance y from central layer and the stress in this fibre is:

$$\varepsilon = \frac{\pm(\rho + y)\cdot\theta - \rho\cdot\theta}{\rho\cdot\theta} = \pm\frac{y}{\rho}, \qquad \sigma_n = \sigma_g - \sigma_c = \pm\frac{y}{\rho}\cdot E - \frac{P}{A} \tag{2}$$

where: ρ – the radius of the curved central line,
θ – angle of the central line slope in relation to the forces line (Fig. 1),
E – Young's modulus of elasticity of a shell,
P – axial force,
A – area of the critical cross-section.

Due to the equilibrium of forces:

$$dP = (\sigma_g + \sigma_c)\cdot dA = \left(\pm\frac{y}{\rho}\cdot E - \frac{P}{A}\right)\cdot dA, \quad \frac{E}{\rho}\int_A(\pm y)\cdot dA = P\int_A\frac{dA}{A}$$

$$\frac{E}{\rho}\cdot 2\cdot S_x^{A/2} = P\cdot\ln(A) \tag{3}$$

where $S_x^{A/2}$ is the static moment. Because:

$$\frac{1}{\rho} \approx \frac{d^2y}{dx^2} = P \cdot \frac{\ln(A)}{2 \cdot S_x^{A/2} \cdot E} \tag{4}$$

then the differential equation of the deflection curve and of its slope and equation of the deflection curve for rods axially compressed with forces by balls (the boundary conditions: $dy/dx = 0$, when $x = L/2$ and $y = 0$, when $x = 0$) are:

$$\frac{2 \cdot S_x^{A/2} \cdot E}{\ln(A)} \cdot \frac{d^2y}{dx^2} = P, \quad \frac{2 \cdot S_x^{A/2} \cdot E}{\ln(A)} \cdot \frac{dy}{dx} = P \cdot \left(x - \frac{L}{2} \right)$$

$$\frac{2 \cdot S_x^{A/2} \cdot E}{\ln(A)} \cdot y = \frac{P}{2} \cdot x \cdot (x - L) \tag{5}$$

where: R – the median tube radius,
t – wall thickness,
L – tube length.

And for rods axially compressed with force with one end fixed (the boundary conditions: $dy/dx = 0$, when $x = L$ and $y = 0$, when $x = 0$) are:

$$\frac{2 \cdot S_x^{A/2} \cdot E}{\ln(A)} \cdot \frac{d^2y}{dx^2} = P, \quad \frac{2 \cdot S_x^{A/2} \cdot E}{\ln(A)} \cdot \frac{dy}{dx} = P \cdot (x - L)$$

$$\frac{2 \cdot S_x^{A/2} \cdot E}{\ln(A)} \cdot y = P \cdot x \cdot \left(\frac{x}{2} - L \right) \tag{6}$$

From the assumption, that the losing of carrying capacity follows when the force line exit outside the critical transverse section ($y_{x=L/2} = y_{cr} = R$), the critical stress for rods axially compressed with forces by balls is equal to:

$$\sigma_{cr}^{E} = \frac{16 \cdot S_x^{A/2} \cdot E}{A \cdot L^2 \cdot \ln(A)} \cdot y_{cr} \tag{7}$$

and for rods axially compressed with force with one end fixed:

$$\sigma_{cr}^{E} = \frac{4 \cdot S_x^{A/2} \cdot E}{A \cdot L^2 \cdot \ln(A)} \cdot y_{cr} \tag{8}$$

The main conclusion of the function (7) showed on Figure 3 or the function (8) showed on Figure 4 is, that to determine σ_{cr}^{E} for all cases of cylindrical shapes is not enough relate them only to the slenderness ratio λ, but we must relate them to A too, because for the same slenderness ratio λ (like in the Euler's formula) we may get different values of σ_{cr}^{E} (depending on A). The analysis of the theoretical results shows, that the simplifications of this theory (taking into consideration only normal stresses, the assumption of flat cross-sections and little slope) cause the limits of use it in an engineering practice. One of the limits for cylindrical shell is $A > 1.00$ m^2, because in that case the functions (7) and (8) are asymptotic going to flat plane $A = 1.00$ m^2. Because all phenomenon proceed in elastic states then a slenderness ratio $\lambda > \lambda_{ltd}$.

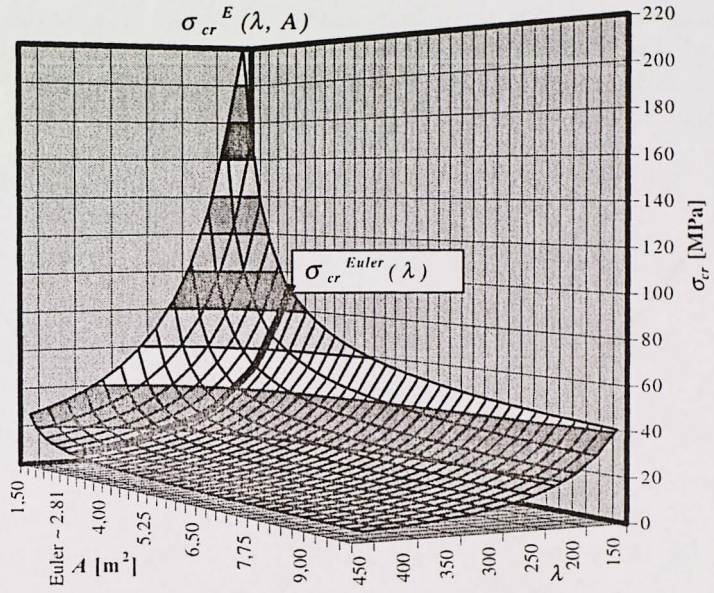

Fig. 3. The surface function $\sigma_{cr}^{E}(\lambda, A)$ of the cylindrical shells made of steel compressed with forces by balls

Rys. 3. Funkcja powierzchniowa $\sigma_{cr}^{E}(\lambda, A)$ dla powłok cylindrycznych wykonanych ze stali ściskanych siłami przez kule

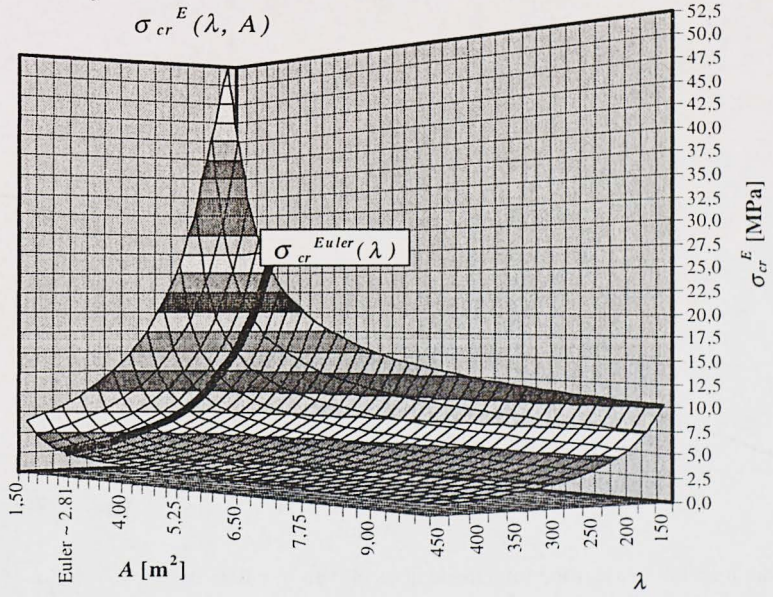

Fig. 4. The surface function $\sigma_{cr}^{E}(\lambda, A)$ of the cylindrical shells made of steel with one end fixed

Rys. 4. Funkcja powierzchniowa $\sigma_{cr}^{E}(\lambda, A)$ dla powłok cylindrycznych wykonanych ze stali z utwierdzonym jednym końcem

Nevertheless below (Fig. 5–10) is presented the stability analysis (the deflection curve $y(x)$, its slope dy/dx, the dependence $y_{L/2}(P)$) of the tube with $R = 0.95$ m, $t = 0.3$ m, $L = 150$ m, $A = 1.791$ m^2 as the theoretical example. Assumed the Young's modulus $E = 210\,000$ MPa.

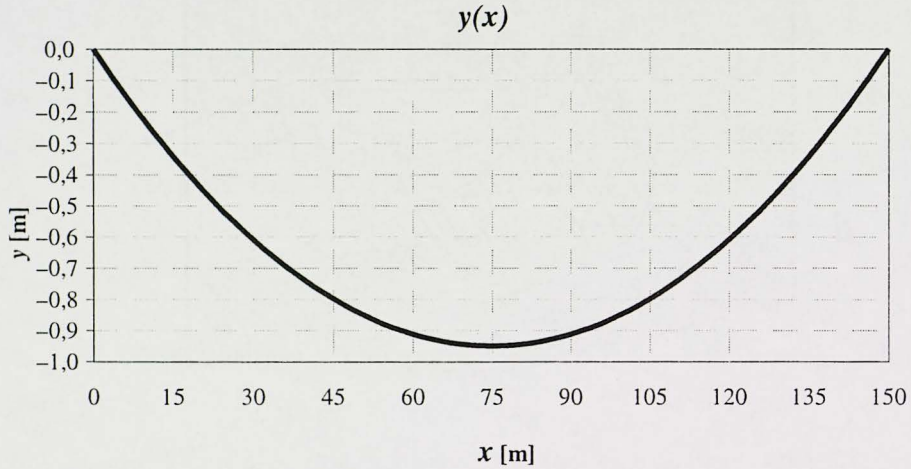

Fig. 5. The function $y(x)$ of the tube made of steel with $R = 0.95$ m, $t = 0.3$ m, $L = 150$ m compressed with forces by balls

Rys. 5. Funkcja $y(x)$ dla rury ze stali o $R = 0{,}95$ m, $t = 0{,}3$ m, $L = 150$ m ściskanej siłami przez kule

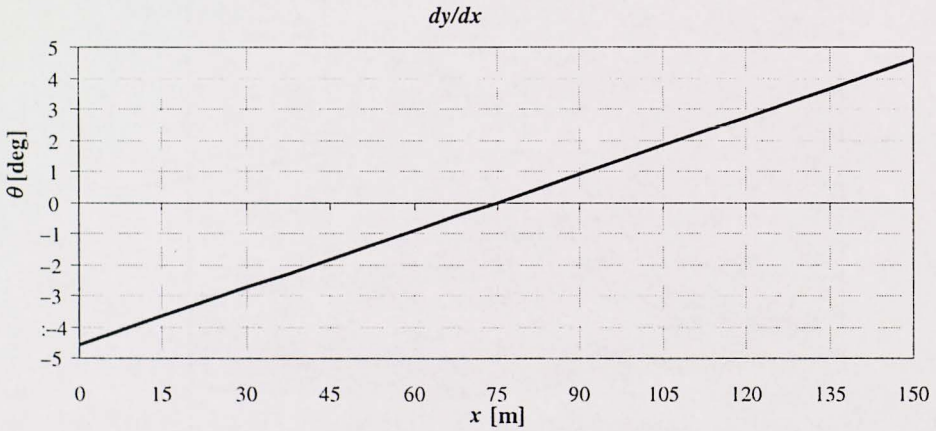

Fig. 6. The function dy/dx of the tube made of steel with $R = 0.95$ m, $t = 0.3$ m, $L = 150$ m compressed with forces by balls

Rys. 6. Funkcja dy/dx dla rury ze stali o $R = 0{,}95$ m, $t = 0{,}3$ m, $L = 150$ m ściskanej siłami przez kule

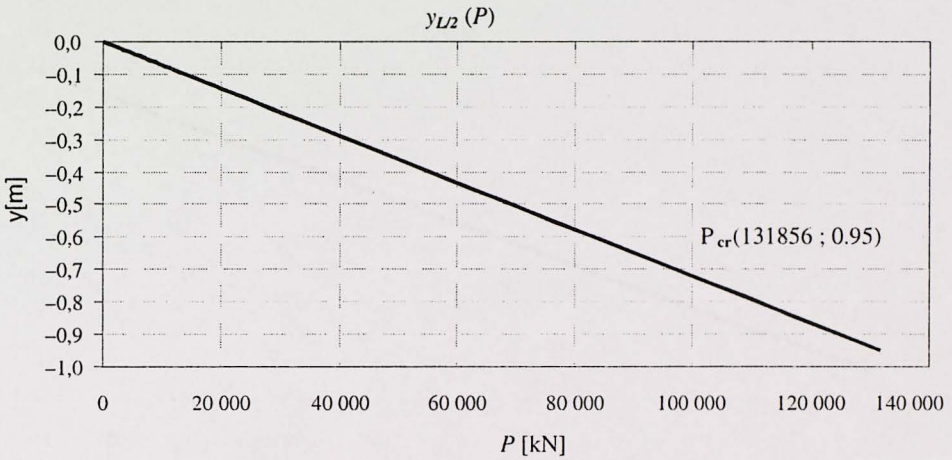

Fig. 7. The function $y_{L2}(P)$ of the tube made of steel with $R = 0.95$ m, $t = 0.3$ m, $L = 150$ m compressed with forces by balls

Rys. 7. Funkcja $y_{L2}(P)$ dla rury ze stali o $R = 0{,}95$ m, $t = 0{,}3$ m, $L = 150$ m ściskanej siłami przez kule

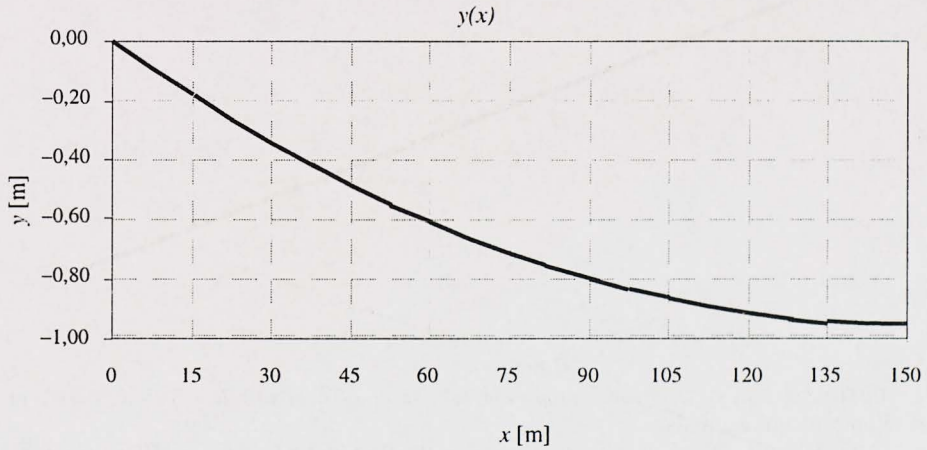

Fig. 8. The function $y(x)$ of the compressed tube made of steel with $R = 0.95$ m, $t = 0.3$ m, $L = 150$ m with one end fixed

Rys. 8. Funkcja $y(x)$ dla ściskanej rury ze stali o $R = 0{,}95$ m, $t = 0{,}3$ m, $L = 150$ m utwierdzonej w jednym końcu

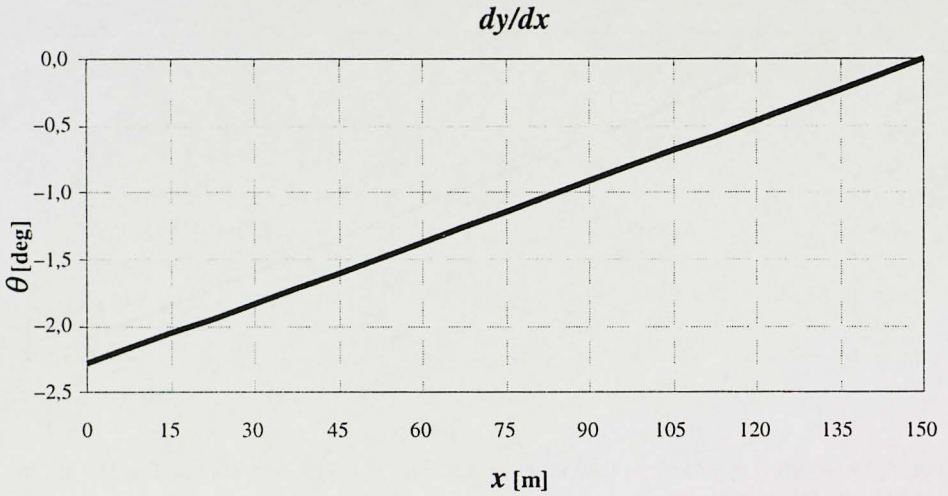

Fig. 9. The function dy/dx of the compressed tube made of steel with R = 0.95 m, t = 0.3 m, L = 150 m with one end fixed
Rys. 9. Funkcja dy/dx dla ściskanej rury ze stali o R = 0,95 m, t = 0,3 m, L = 150 m utwierdzonej w jednym końcu

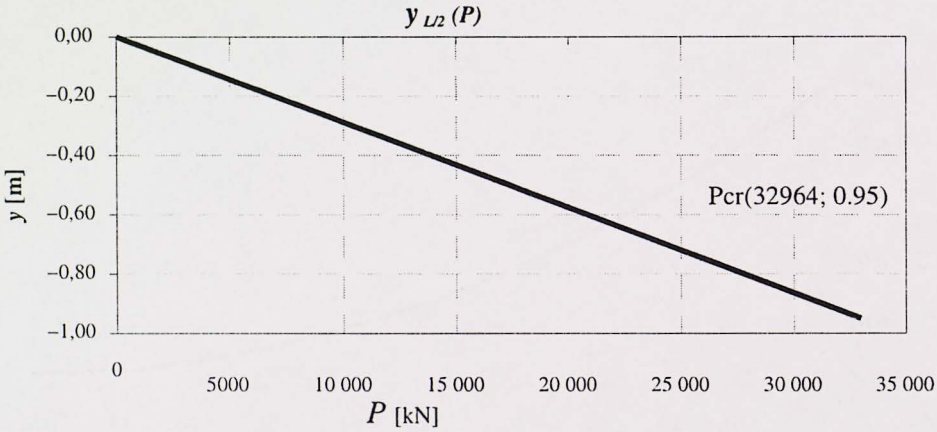

Fig. 10. The function $y_{L2}(P)$ of the compressed tube made of steel with R = 0.95 m, t = 0.3 m, L = 150 m with one end fixed
Rys. 10. Funkcja $y_{L2}(P)$ dla ściskanej rury ze stali o R = 0,95 m, t = 0,3 m, L = 150 m utwierdzonej w jednym końcu

The cylindrical shell axially compressed by balls

For the cylindrical shell axially compressed by balls the functions for the deflection curve $y(x)$, its slope dy/dx and the dependence $y_{L2}(P)$, according to (5) and (7), are:

$$\frac{4 \cdot E \cdot R^2 \cdot t}{\ln(2 \cdot \pi \cdot R \cdot t)} \cdot y = \frac{P}{2} x \cdot (x - L), \quad \frac{4 \cdot E \cdot R^2 \cdot t}{\ln(2 \cdot \pi \cdot R \cdot t)} \cdot \frac{dy}{dx} = P \cdot \left(x - \frac{L}{2} \right)$$

$$y_{L/2} = -\frac{\ln(2 \cdot \pi \cdot R \cdot t)}{E \cdot R^2 \cdot t} \cdot \frac{L^2}{32} \cdot P \tag{9}$$

$$\sigma_{cr}^{E} = \frac{32 \cdot E}{\lambda^2 \cdot \pi \cdot \ln(2 \cdot \pi \cdot R \cdot t)} \tag{10}$$

In case of the example: $\lambda = 220.6$ and $\sigma_{cr}^{Euler}(\lambda) = 42.603$ MPa but $\sigma_{cr}^{E}(\lambda, A) = 73.633$ MPa.

We see on graphs in Figure 3 and 4, that $\sigma_{cr}^{Euler}(\lambda) \approx \sigma_{cr}^{E}(\lambda, A)$ for A [m^2] = 2,8068114. Hence for A [m^2] < 2,8068114 is $\sigma_{cr}^{Euler}(\lambda) < \sigma_{cr}^{E}(\lambda, A)$ and for A [m^2] > 2,8068114 is $\sigma_{cr}^{Euler}(\lambda) > \sigma_{cr}^{E}(\lambda, A)$.

The cylindrical shell compressed axially with one end fixed

For the cylindrical shell compressed axially with one end fixed, the functions for the deflection curve $y(x)$, its slope dy/dx and the dependence $y_{L/2}(P)$, according to (6) and (8), are:

$$\frac{4 \cdot E \cdot R^2 \cdot t}{\ln(2 \cdot \pi \cdot R \cdot t)} \cdot \frac{dy}{dx} = P \cdot (x - L), \quad \frac{4 \cdot E \cdot R^2 \cdot t}{\ln(2 \cdot \pi \cdot R \cdot t)} \cdot y = P \cdot x \cdot \left(\frac{x}{2} - L \right)$$

$$y_{L/2} = -\frac{\ln(2 \cdot \pi \cdot R \cdot t)}{E \cdot R^2 \cdot t} \cdot \frac{L^2}{8} \cdot P \tag{11}$$

$$\sigma_{cr}^{E} = \frac{8 \cdot E}{\lambda^2 \cdot \pi \cdot \ln(2 \cdot \pi \cdot R \cdot t)} \tag{12}$$

In case of the example: $\sigma_{cr}^{Euler}(\lambda) = 10.651$ MPa but $\sigma_{cr}^{E}(\lambda, A) = 18.408$ MPa.

STRESSES AND STRAINS ANALYSIS

Assumed, that the state of strains, is as a result of a superposition of bending and pure compression and the losing of a carrying capacity in elastic states follows when the resultant neutral layer exit outside the critical transverse section (Fig. 1 and 2):

$$\varepsilon_n \cdot E = \sigma_n = \sigma_g + \sigma_c = \pm \frac{y}{\rho} \cdot E - \frac{P}{A} = E \cdot \left(\pm \frac{y}{\rho} - \frac{\Delta L}{L} \right) = E \cdot (\pm \varepsilon_g - \varepsilon_c) \Rightarrow$$

$$\Rightarrow \varepsilon_n = \pm \varepsilon_g - \varepsilon_c \tag{13}$$

where: σ_g – the bending stress,
σ_c – compression stress,
σ_y – orthogonal stress,
ε_g – bending strain,
ε_c – compression strain,
ε_y – orthogonal strain.

Due to the equilibrium of moments:

$$M_b = \int dP \cdot y = \iint \left(\pm \frac{y}{\rho} \cdot E - \frac{P}{A} \right) dA \cdot y \quad \text{and} \quad M_b = \frac{E}{\rho} \cdot J_x - P \cdot \int_A y \cdot \frac{dy}{A} \tag{14}$$

where: M_b – the bending moment,
J_x – moment of inertia of cross-section area.

Hence the stress σ_n equals:

$$\sigma_n = \sigma_g - \sigma_c = \frac{M_b}{J_x} \cdot y - \frac{P}{A} \tag{15}$$

The formulas for σ_c, σ_g, ε_g and ε_c caused by external load or σ_y and ε_y caused with ν (Poisson's ratio) by internal load, are like follows:

$$\sigma_c(x, y) = \frac{\sigma_g}{\sqrt{1 + \left(\frac{dy}{dx} \right)^2}} \approx \sigma_g(x, y), \quad \sigma_y(x, y) \approx -\sigma_n \cdot \nu \tag{16}$$

$$\varepsilon_n(x, y) = \frac{\sigma_n(x, y)}{E}, \quad \varepsilon_c(x, y) = \frac{\varepsilon_g}{\sqrt{1 + \left(\frac{dy}{dx} \right)^2}} \approx \varepsilon_g(x, y), \quad \varepsilon_y(x, y) = -\varepsilon_n \cdot \nu \tag{17}$$

The analysis of the theoretical results shows, that the simplifications of this theory (the assumption of flat cross-sections planes and little slope) cause the limits of use it in an engineering practice. Nevertheless below (Fig. 11–18) is presented the stresses and strains analysis in the cylindrical shell (depending on x and y, where $x = 0 \div L$ and $y = -1R, -0.5R, -0.1R, 0.0, 0.1R, 0.5\,R, 1R$) as the theoretical example (assumed: $\nu = 0.3$).

The cylindrical shell axially compressed by balls

For the cylindrical shell axially compressed by balls depending on x and y:

$$\sigma_n(x, y) = \frac{y \cdot x \cdot (x - L) \cdot \ln(2 \cdot \pi \cdot R \cdot t) \cdot P^2}{8 \cdot \pi \cdot E \cdot R^5 \cdot t^2} - \frac{P}{2 \cdot \pi \cdot R \cdot t} \tag{18}$$

The cylindrical shell compressed axially with one end fixed

For the cylindrical shell compressed axially with one end fixed depending on x and y:

$$\sigma_n(x,y)=\frac{y\cdot x\cdot\left(\frac{x}{2}-L\right)\cdot\ln(2\cdot\pi\cdot R\cdot t)\cdot P^2}{4\cdot\pi\cdot E\cdot R^5\cdot t^2}-\frac{P}{2\cdot\pi\cdot R\cdot t} \tag{19}$$

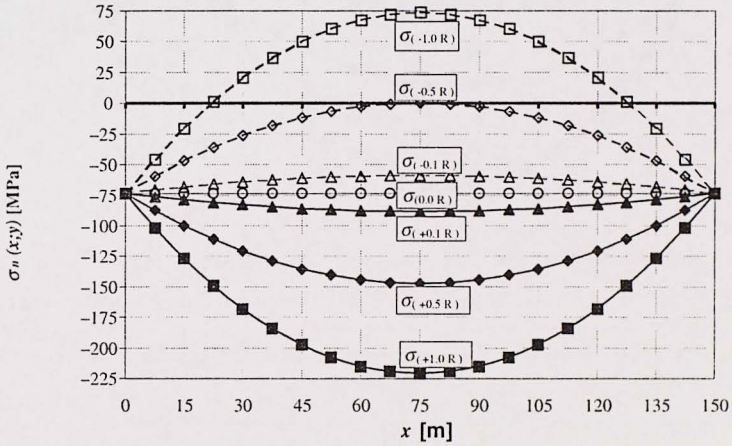

Fig. 11. Stresses $\sigma_n(x, y)$ of the tube made of steel with R = 0.95 m, t = 0.3 m, L = 150 m compressed with forces by balls

Rys. 11. Naprężenia $\sigma_n(x, y)$ dla rury ze stali o R = 0,95 m, t = 0,3 m, L = 150 m ściskanej siłami przez kule

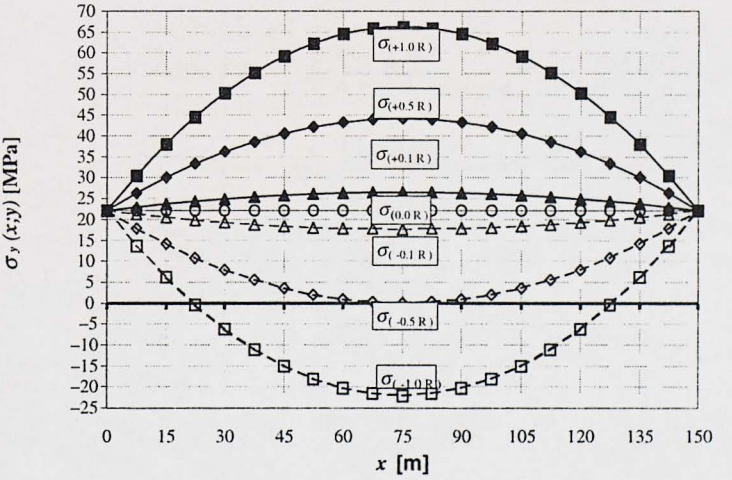

Fig. 12. Stresses $\sigma_y(x, y)$ of the tube made of steel with R = 0.95 m, t = 0.3 m, L = 150 m compressed with forces by balls

Rys. 12. Naprężenia $\sigma_y(x, y)$ dla rury ze stali o R = 0,95 m, t = 0,3 m, L = 150 m ściskanej siłami przez kule

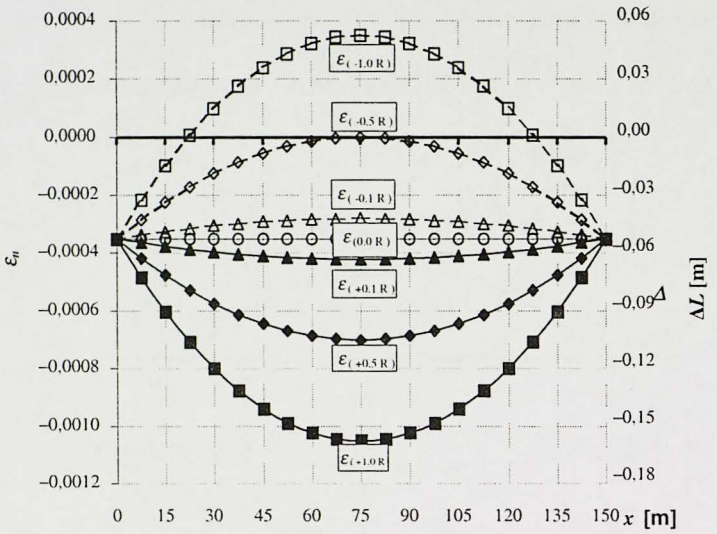

Fig. 13. Strains $\varepsilon_n(x, y)$ of the tube made of steel with $R = 0.95$ m, $t = 0.3$ m, $L = 150$ m compressed with forces by balls

Rys. 13. Odkształcenia względne $\varepsilon_n(x, y)$ dla rury ze stali o $R = 0{,}95$ m, $t = 0{,}3$ m, $L = 150$ m ściskanej siłami przez kule

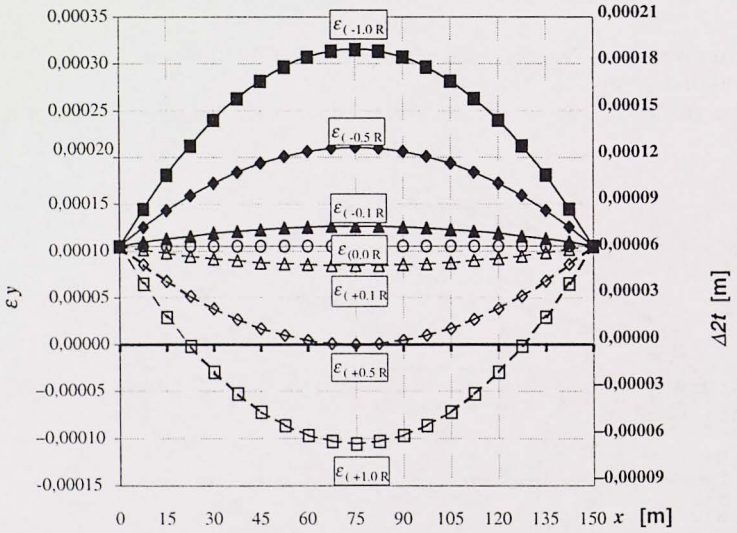

Fig. 14. Strains $\varepsilon_y(x, y)$ of the tube made of steel with $R = 0.95$ m, $t = 0.3$ m, $L = 150$ m compressed with forces by balls

Rys. 14. Odkształcenia względne $\varepsilon_y(x, y)$ dla rury ze stali o $R = 0{,}95$ m, $t = 0{,}3$ m, $L = 150$ m ściskanej siłami przez kule

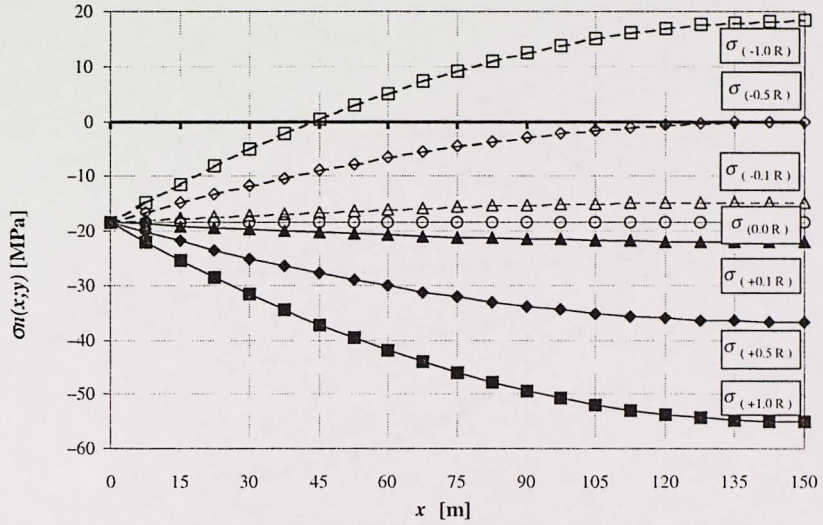

Fig. 15. Stresses $\sigma_n(x, y)$ of the compressed tube made of steel with $R = 0.95$ m, $t = 0.3$ m, $L = 150$ m with one end fixed

Rys. 15. Naprężenia $\sigma_n(x, y)$ dla ściskanej rury ze stali o $R = 0{,}95$ m, $t = 0{,}3$ m, $L = 150$ m utwierdzonej w jednym końcu

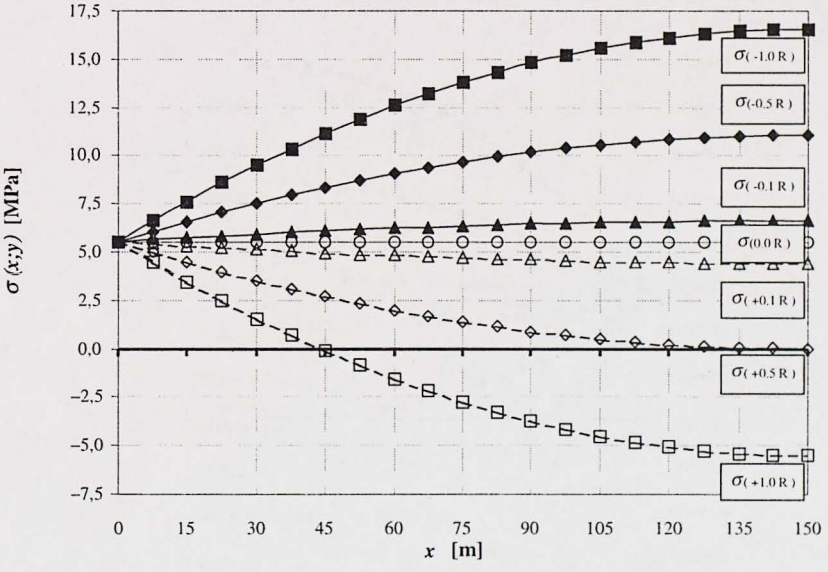

Fig. 16. Stresses $\sigma_y(x, y)$ of the compressed tube made of steel with $R = 0.95$ m, $t = 0.3$ m, $L = 150$ m with one end fixed

Rys. 16. Naprężenia $\sigma_y(x, y)$ dla ściskanej rury ze stali o $R = 0{,}95$ m, $t = 0{,}3$ m, $L = 150$ m utwierdzonej w jednym końcu

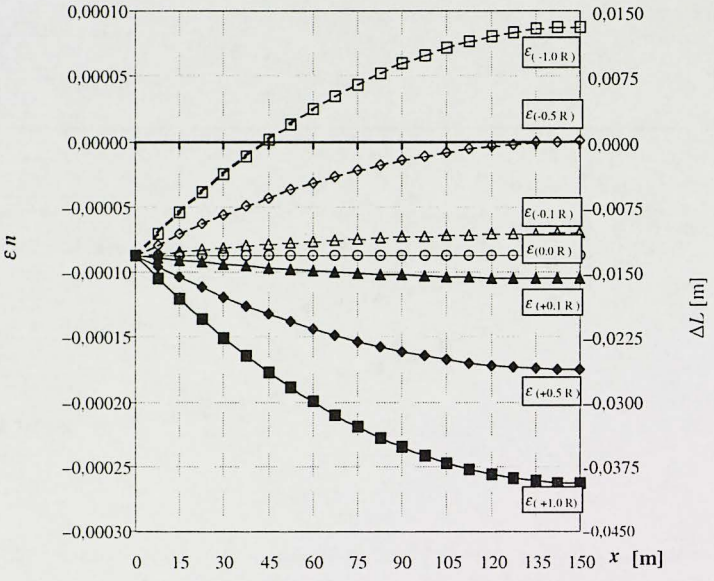

Fig. 17. Strains $\varepsilon_n(x, y)$ of the compressed tube made of steel with $R = 0.95$ m, $t = 0.3$ m, $L = 150$ m with one end fixed

Rys. 17. Odkształcenia względne $\varepsilon_n(x, y)$ dla ściskanej rury ze stali o $R = 0{,}95$ m, $t = 0{,}3$ m, $L = 150$ m utwierdzonej w jednym końcu

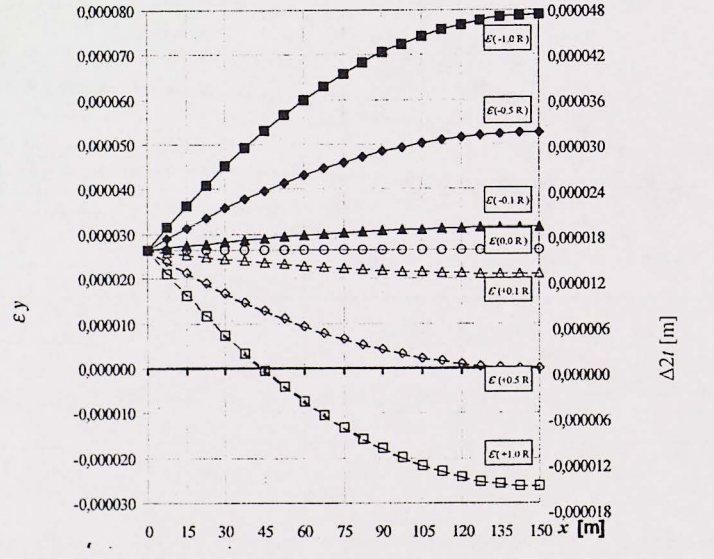

Fig. 18. Strains $\varepsilon_y(x, y)$ of the compressed tube made of steel with $R = 0.95$ m, $t = 0.3$ m, $L = 150$ m with one end fixed

Rys. 18. Odkształcenia względne $\varepsilon_y(x, y)$ dla ściskanej rury ze stali o $R = 0{,}95$ m, $t = 0{,}3$ m, $L = 150$ m utwierdzonej w jednym końcu

CONCLUSIONS

On the basis of the Euler's formula we can determine a critical stress but we cannot determine shell stresses or strains during losing stability of axially compressed rod. This is possible using elastic stability theory of Timoshenko or Finite Element Theory (FEM) based on Euler's theory.

Presented in the paper theory gives possibility to determine in elastic states a critical stress, equations of the deflection curve and its slope, shell strains and stresses of axially compressed rod. Due to different concept results are different in relation to results of Euler's theory.

REFERENCES

Bleich F., 1952. Buckling strength of metal structures. McGraw-Hill Book Company, Inc. New York, Toronto, London.

Březina V., 1966. Stateczność prętów konstrukcji metalowych. Arkady, Warszawa.

Considère A., 1889. Resistance des pièces comprimèes. Congrès international de procedès de costruction (op. cit.).

Euler L., 1744. Methodus inveniendi lineas curves maximi minimive proprietate gaudentes. Appendix 1. De curvis elasticis (in Latin). Lausanne and Geneva (op.cit.).

Euler L., 1759. Sur la force de colonnes (in French). Memoires de l'Academie de Berlin, 13, 251–282. (op. cit.).

Grashof F., 1878. Theorie der Elasticität und Festigkeit. Berlin (op. cit.).

Grygoliuk E., Kabanow B.B., 1987. Ustojcziwost obołoczek. Lieningrad.

Murawski K., 1992. Stability of thin shell columns in elasto-plastic states. 14 Międzynarodowe Sympozjum Naukowe Studentów i Młodych Pracowników Nauki. Mechanika. Zielona Góra.

Murawski K., 1998. Modelowanie procesu pochłaniania energii w warstwowych zderzakach. Praca doktorska. Wydział Maszyn Roboczych i Pojazdów, Politechnika Poznańska.

Murawski K., 2002. The Engesser-Shanley modified theory of thin-walled cylindrical rods with example of use for steel St35. Acta Scientarum Polonorum. Architectura 1–2 (1–2), 85–95.

Reese S., Wriggers P., 1995. A Finite-Element Method for Stability Problems in Finite Elasticity. Int. Journal for Numerical Methods in Engineering, 38, 7, 1171–1200.

Salmon E.H., 1921. Columns. Oxford Technical Publication, London.

Timoshenko S.P., Gere J.M., 1963.Teoria stateczności sprężystej. Arkady, Warszawa.

Weiss S., Giżejowski M., 1991. Stateczność konstrukcji metalowych. Układy prętowe. Arkady, Warszawa.

Wolmir A. C., 1967. Ustojcziwost dieformirujemych sistiem. Nauka, Moskwa.

Życzkowski M., 1981. Podstawy analizy stateczności prętów sprężystych. Współczesne metody analizy stateczności konstrukcji. Ossolineum, Wrocław.

ZMODYFIKOWANA TEORIA STATECZNOŚCI EULERA Z ANALIZĄ NAPRĘŻEŃ I ODKSZTAŁCEŃ NA PRZYKŁADZIE BARDZO SMUKŁYCH CYLINDRYCZNYCH POWŁOK WYKONANYCH ZE STALI

Streszczenie. W pracy przedstawiono teorię stateczności osiowo ściskanej cylindrycznej powłoki. Autor przeanalizował równanie różniczkowe osi ugięcia i jej nachylenia, krytycznych naprężeń, naprężeń i odkształceń w powłoce bardzo smukłych rur w stanach sprężystych przy założeniu hipotezy płaskich przekrojów i małych ugięć osi ugięcia. Otrzymane teoretyczne wyniki krytycznych naprężeń odniesiono do smukłości kształtki oraz do pola przekroju poprzecznego cylindrycznej powłoki, a teoretyczne wyniki wartości naprężeń i odkształceń dla przykładowej rury ze stali przedstawiono na wykresach.

Słowa kluczowe: stateczność, Euler, naprężenie krytyczne, bardzo smukła, cylindryczna powłoka

K. Murawski, Akademia Rolnicza w Poznaniu, Wydział Technologii Drewna, Zakład Obrabiarek i Podstaw Konstrukcji Maszyn, ul. Wojska Polskiego 38/42, 60-627 Poznań
e-mail: kmurawski@woodcock.au.poznan.pl